Geothermally Sourced Combined Power and Freshwater Generation for Eastern Africa

Neil M. Burnside[1*], Sham Rane[2], Guopeng Yu[1], Haiteng Ma[2,3], Nelly Montcoudiol[1], Weihong Li[1], Elias Lewi Teklemariam[4], Adrian Boyce[5], Li He[2], & Zhibin Yu[1].

[1] School of Engineering, University of Glasgow, UK

[2] Oxford Thermofluids Institute, University of Oxford, UK

[3] School of Mechanical Engineering, Shanghai Jiao Tong University, China

[4] Arat Kilo Campus Institute of Geophysics, Addis Ababa University, Ethiopia

[5] Scottish Universities Environmental Research Centre (SUERC), East Kilbride, UK

*neil.burnside@glasgow.ac.uk

Keywords: Power, Water, Innovation, East Africa.

ABSTRACT

The Geothermally Sourced Combined Power and Freshwater Generation for Eastern Africa (Combi-Gen) project aims to deliver enhanced power and water resource capabilities to energy-poor and water-scarce nations associated with the East African Rift System (EARS). The Combi-Gen project utilises a robust understanding of geothermal resources and develops a novel thermal chimney driven air-cooled condenser coupled to Trilateral Flash Cycle power generation. This whole systems approach allows for development of a system that produces power and fresh water with no parasitic power load. This paper reports our initial data assessment and modelling results which showcase optimal thermal exchange efficiency parameters and engineering system design.

1. INTRODUCTION

Water is essential for life; however, by 2025 half of the world's population will be living in areas where water quality and availability is under constant stress (WHO 2015). This is a particularly acute issue in those tectonically active zones that occur in arid to semi-arid regions, many of which also host some of the largest, and most rapidly expanding, populations on Earth. The EARS spans some of the world's most deprived countries, where widespread poverty, potable water scarcity and a chronic lack of access to sustainable, safe energy are endemic. Geothermal energy is vastly under-utilised in the EARS and represents an exciting means of addressing energy and water challenges and promoting economic development. Thanks to the effects of sustained geological rifting, both Ethiopia and Kenya each have estimated total geothermal resources of ~ 10 GW (Kagiri 2014; Tibetu 2018). Geothermal exploration is currently underway in the area around Fantale, Ethiopia, with a view to developing a power plant of greater than 100 MWe capacity (Hotspur 2015), and ultimately power generation on a scale of 100's of MW. Kenya's geothermal capabilities are more developed, with an installed capacity of 673 MW at the end of 2017 (IRENA, 2019) supplying 43% of total electricity generation in 2016 (IEA 2019), and an ambitious national target of 5 GW by 2030 (Kenyan Government 2014).

Initiatives to address concurrent water and energy issues have largely been pursued separately; yet geothermal sources can provide both power and fresh water to maximise the benefit to the poorest populations, provided suitable technologies are available. However, the exploitation of geothermal sources has so far focused almost entirely on power generation, with the extracted geothermal water either reinjected into the geothermal reservoir or discharged to the environment in the form of co-produced brine and / or uncondensed steam. The condensation of steam offers a direct opportunity to significantly augment local freshwater sources, through a zero-carbon and renewable equivalent of the flash distillation process that has allowed the oil states of the Middle East to flourish in recent decades (Reddy and Ghaffour 2007). The Combi-Gen project aims to develop a novel geothermally sourced combined power and fresh water generation technology which promises to initiate a genuinely disruptive shift in the engineering response to the twin challenges of energy shortage and water-scarcity.

The Combi-Gen concept is based on Trilateral Flash Cycle power generation, but with several key features to enhance practicality for geothermal application and eliminate parasitic power requirements, including a two-phase reaction turbine to partially flash geothermal water into vapour and a novel thermal chimney driven air-cooled condenser to produce fresh water. This development of a new geothermal energy conversion cycle will take place within a comprehensive responsible-innovation framework (e.g. Owen et al. 2012), with the end goal of

addressing a range of societal and environmental issues.

2. EARS GEOTHERMAL LOCATIONS

The focus of Combi-Gen is on the nations of the East African Rift System (EARS), which runs north-to-south from Eritrea to Mozambique, covering a total of 11 countries. Rift extension here has led to a thinning of the Earth's crust and allows for hot buoyant magma to rise closer to the surface, resulting in the manifestation of numerous volcanic features and superheated groundwater systems (Lysak 1992). The high enthalpy groundwaters associated with this process provide a large potential geothermal resource and an exciting opportunity to develop low-carbon energy.

Figure 1: Satellite image of Aluto-Langano volcanic complex (from Google Earth) showing surface water features and location of geothermal drilling activity (coloured circles). Red- productive wells; Green- reinjection well; Blue- non-productive wells (all from Teklemariam & Beyene 2001); and Black with red outline- newly-drilled directional wells (from Biru 2016).

In order to ensure sustainable development of these geothermal resources we must have a firm understanding of the wider hydrogeological systems within which they exist. In addition, technically appealing subsurface abstraction points must be reconciled with existing surface infrastructure for both energy and water provision. Our main focus is on low-cost and efficient characterisation of hydrological parameters of surface and ground waters (Burnside et al. 2016) in areas of particular interest to Combi-Gen technology application. Hydrochemical assessment of these waters allows for a robust understanding of the geothermal fluids that will provide the fuel for power generation and can be used to identify key indicators for the environmental sensitivity of geothermal resource development. Determinants include: (a) in-situ physico-chemical parameters (T, Eh, pH); (b) major and trace solutes indicative of geothermal dynamics (Younger 2010); and (c) stable isotopes of O, H, C and S. Of particular interest in such assessments is the volume of dissolved silica, both as an indicator of maximum temperatures in deep geothermal reservoirs and as an early-warning variable for potential scaling of engineered infrastructure.

The focus of fieldwork within the Combi-Gen project is Kenya and Ethiopia. Analyses of Kenya-related field efforts within the Gregory Rift Segment of the EARS are currently under review for integration with modelling and experimental assessment of Combi-Gen technology (Sections 3, 4 and 5). Addis Ababa University led fieldwork is currently underway to provide further assessment of the area around Fantale, Ethiopia, where geothermal exploration is currently underway. Published data from the Aluto-Langano field (Geremew 2012) was used for initial modelling investigations of the Combi-Gen thermal chimney and turbine technologies.

Initial exploration at Aluto-Langano took place from 1981-1986 with the drilling of eight deep exploratory wells (LA-1 to LA-8), four of which were found to be productive (LA-3, LA-4, LA-6 and LA-8) (Teklemariam & Beyene 2001). Development took place in the 90's and culminated with the construction of a pilot power plant and generation of electricity by 1998 (IEA 2019). The exploitation was based on the use of the four productive exploration wells and a fifth reinjection well (LA-7; Figure 1). Geothermal energy production ceased from 2002-2007 due to operational issues (Biru 2016). Since 2012, the plant has been producing less than 1 MW per year, just enough for self-sufficiency (Tadesse 2018). As part of an expansion plan, two new directional wells were drilled in 2013-2015 (Figure 1). Production testing suggests that each of these wells could potentially produce 2.9 - 3.8 MWe of electric power output (Biru 2016).

3. DISTRIBUTED-PARAMETER MODEL OF THE COMBI-GEN SYSTEM

The proposed Combi-Gen technology is shown in Figure 2. A flow of high temperature geothermal water passes a self-designed two-phase reaction turbine and partially flashes into vapour. It spins the turbine, and subsequently the generator, to produce power, and then the vapour can be condensed to produce freshwater.

In order to illustrate the effects of distributed-parameters on system performance, select appropriate heat source and provide guidelines for lab-scaled system design, construction and experiments, the proposed system was first modelled as a trilateral cycle for 1kW power generation and fresh water generation taking geothermal water as heat source.

Five wells from the Aluto-Langano geothermal field in Ethiopia were considered (Geremew 2012) and five additional geothermal source temperatures (200°C, 180°C, 160°C, 140°C and 120°C), which are more

realistic for future lab experimentation, were also included in simulations (Table 1).

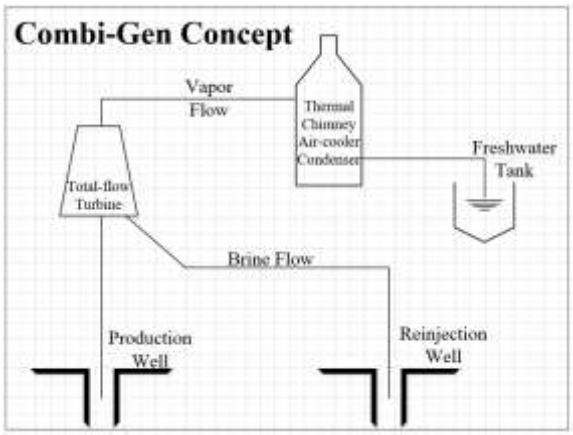

Figure 2: Schematic of the Combi-Gen system

The performance of the proposed system was assessed by assuming that the turbine has different isentropic efficiencies, ranging from 1% to 50%, for each scenario. A pinch point temperature difference (PPTD) method was adopted during the heat transfer process for the heat exchangers. The PPTD of the condenser was set as 30 °C, the ambient temperature (T_0) was assumed to be 30 °C, and the condensation temperature (T_{cond}) was set at 100 °C to avoid vacuum and flow-back. Figure 3 and Table 1 give the basic process, thermal points and pre-set parameters for the modelling studies.

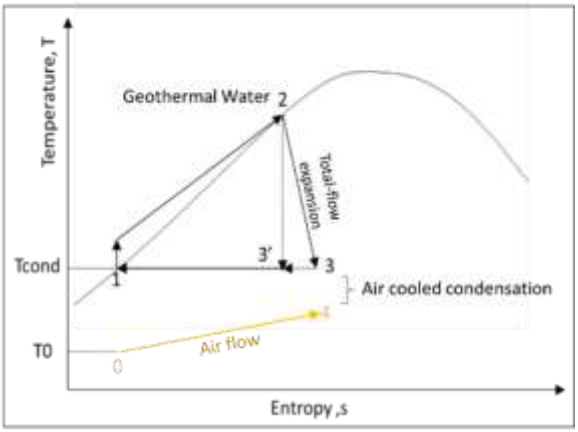

Figure 3: Temperature vs. entropy plot of the thermal process for system simulation

Table 1: Pre-set parameters for system modelling. Well data from Geremew (2012)

Heat source	Parameter	Unit	Value
Well LA-6	T_2 / P_2	°C/bar	329.0 /126.9
Well LA-3	T_2 / P_2	°C/bar	312.8 /102.5
Well LA-8	T_2 / P_2	°C/bar	269.0 /54.2
Well LA-4	T_2 / P_2	°C/bar	234.0 /30.1
Well LA-7	T_2 / P_2	°C/bar	219.7 /23.1
Lab-200	T_2 / P_2	°C/bar	200.0 /15.5
Lab-180	T_2 / P_2	°C/bar	180.0 /10.0
Lab-160	T_2 / P_2	°C/bar	160.0 /6.2
Lab-140	T_2 / P_2	°C/bar	140.0 /3.6
Lab-120	T_2 / P_2	°C/bar	120.0 /2.0
	T_1 / P_1	°C/bar	100.0 /1.01
	T_3 / P_3	°C/bar	100.0 /1.01
Ambient condition T_0/P_0		°C/bar	30.0/1.01
Power (target)		kW	1.0

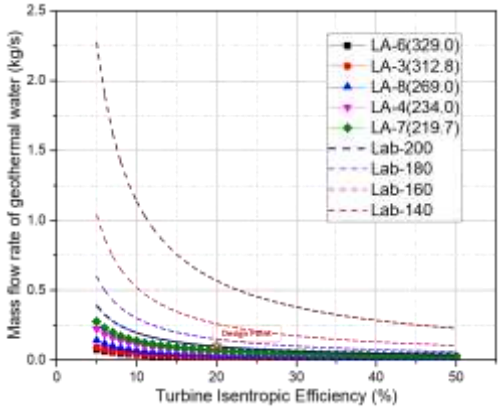

Figure 4: Mass flow rate of the geothermal water vs. Turbine efficiency

Figure 4 shows the mass flow rate of the geothermal water required to generate 1 kW of power. The mass flow rate decreases exponentially as the isentropic efficiency of the two-phase flow turbine increases. It was demonstrated that required water volume has an inverse relationship with source temperature, with the ranking of water quantity required as follows: Lab-140 > Lab-160 > Lab-180 > Lab-200 > LA-7 > LA-4 > LA-8 > LA-3 > LA-6. For the highest temperature LA-6 well, only 0.025 kg/s of geothermal water is required to reach 1 kW generation with a turbine efficiency of 15%. The required volume of geothermal water significantly increases with decreasing temperature, especially for waters below 200 °C. Lab-200 was selected as the design heat source since it is reasonable and achievable for lab investigations. If the turbine efficiency was to reach 20%, the required mass flow rate of this heat source would be 0.098 kg/s.

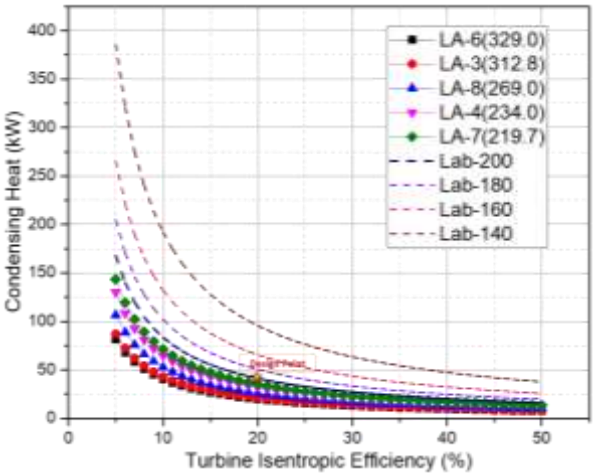

Figure 5: Heat capacity of the condenser vs. Turbine efficiency

The required heat capacity of the condenser would be unreasonably high if the turbine efficiency is too low (Figure 5). Heat capacity requirement has an inverse relationship with the heat source temperature, leading

to stricter requirements for the design of the condenser. For a turbine efficiency of 20%, the LA-6 well requires only 19.6 kW of heat to be condensed, but up to 95.6 kW of heat needs to be condensed for Lab-140. At the design point for Lab-200 the condensing heat required is 41.2 kW.

4. CFD MODELLING OF THERMAL CHIMNEY DRIVEN AIR-COOLED CCONDENSER

A crucial component in Combi-Gen technology is the thermal chimney driven air-cooled condenser, which is responsible for the generation of freshwater from power generation-produced steam. Air flow surrounding the condenser is driven by natural convection, due to its comparatively higher temperature and lower density, and acts as heat transfer enhancement on the external surfaces of the condenser. This process eliminates the need for electric fans and saves energy.

The underlying physical principle for the thermal chimney is natural convection. Therefore, the computational design tool was built up and verified against available published data. In the first instance, the simplest case of natural convection around a single heated cylinder for both laminar and turbulent flow was modelled. Then, in order to analyse the thermal chimney model, a focus was placed on simulating the upward air flow velocity induced by natural draft.

4.1 CFD Setup and Validation

A computational domain, with width 40D and height 20D, was set up with a cylinder at its centre, where D is diameter of the cylinder. Structured mesh was employed with an adequate grid size to resolve the flow field, determined through a mesh independence study. Steady-state simulations were run in ANSYS Fluent using a pressure-based solver and the pressure-velocity coupling scheme was SIMPLEC. Gravity acceleration was set at 9.8 m/s^2 and air properties, such as density, were kept constant.

The lower boundary was set as a pressure inlet with a total pressure (P_t) of 101,325 Pa and a total temperature (T_t) of 293 K. The upper and side boundaries were treated as pressure outlets with a static pressure (P_s) of 101,325 Pa and backflow total temperature of 293 K. Isothermal or isoflux wall boundary conditions were selected for the cylinder surface.

Figure 6 shows a natural convection simulation under a laminar flow regime with Nusselt number distribution from the lowest point ($\theta = 0$) to the highest point ($\theta = 180°$) on the cylinder surface for a Rayleigh number of 10^4. Our CFD results quantitatively match the experimental data by Kuehn and Goldstein (1980) and previous CFD simulations conducted by Saitoh et al. (1993), Wang et al. (1990) and Corcione (2005).

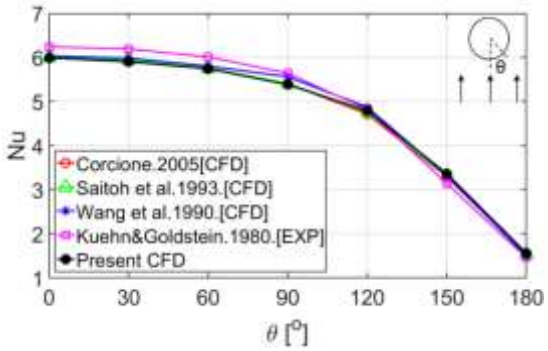

Figure 6: Nusselt number along cylinder surface (natural convection around single heated cylinders, laminar flow model, Ra = 10^4).

For natural convection simulation under a turbulent flow regime, 6 RANS (Reynolds Averaged Navier-Stokes) models (k-ε realizable with enhanced wall treatment, k-ω standard, k-ω SST, transition-k-kl-ω, transition SST and Reynolds stress model) were used and compared with experimental measurements by Grafsrønningen et al. (2011) in water for a Rayleigh number of 7.94x10^7. Figure 7 shows the mean velocity magnitude distribution along the horizontal direction at a vertical location of 3.52D above the cylinder centre. Compared with PIV measurement data from Grafsrønningen et al. (2011), k-ε and Reynolds stress models predict the peak velocity well, with a relative difference within 15%, but with over-predicted plume width. K-ω standard, k-ω SST and transition k-kl-ω models over-predict the peak velocity by 60% and under-estimate the plume width. The transition SST model exhibits the best agreement with experimental data, with velocity deviating by < 25% and a close match with plume width. The transition SST model was therefore selected to simulate turbulence in the rest of the study.

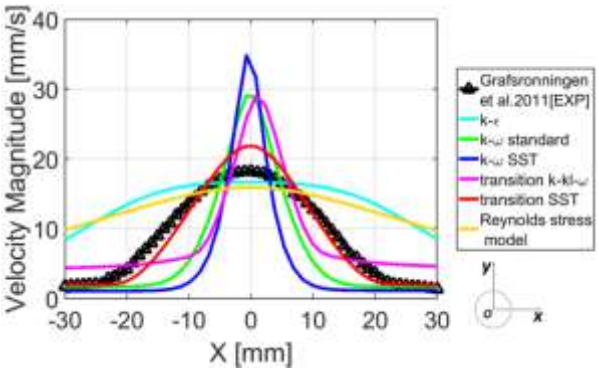

Figure 7: Mean velocity magnitude along x-direction at y=3.52D (RANS models, Ra=7.94x10^7)

4.2 Physical Discovery on Natural Convection Heat Transfer and Fluid Flow

Figure 8a shows the velocity magnitude around a single heated cylinder, using the validated CFD tool for laminar flow. One compelling observation is the acceleration of the thermal plume as it develops downstream. This is contrary to the common understanding that velocity decreases in wakes as it dissipates downstream. As the plume velocity

increases, it becomes unstable at some point and begins to sway, changing from laminar to turbulent flow. This is in line with the experimental measurement by Kitamura et al. (2016), which also reported the swaying motion of thermal plume above a single cylinder. Noto et al. (1999) proposed a criteria to estimate the location where transition to turbulence occurs based on a spectral analysis of a plume emanated from a line-heat-source with the critical point where $Gr_x = \frac{g\beta Q x^3}{v^2 kPr}$=2x10^8. According to this proposition, the transition to turbulence starts at a vertical location of y=9D for Ra = 10^4, which matches well with the observation in Figure 8a. Contours of temperature and total gauge pressure (P_t) are also shown in Figure 8b and Figure 8c. As the thermal plume develops upwards, temperature declines due to heat transfer to the comparatively cold ambient air mass, while total pressure increases, indicating an input of work. This work input is believed to be the result of buoyancy force in the thermal plume region.

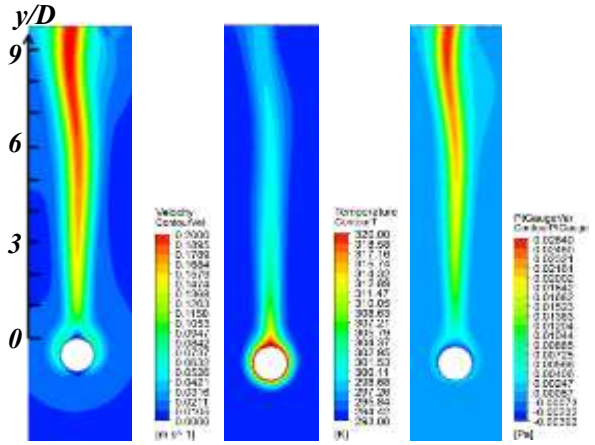

(a) Velocity (b) Temperature (c) Pressure (total, gauge)

Figure 8: Contours of flow variables above a single heated cylinder for Ra = 10^4 (laminar flow model).

4.3 Results and Analysis of the Thermal Chimney Model

The validated CFD procedure served as a basis to model the Combi-Gen thermal chimney for preliminary design purposes. To simplify the design problem into a two-dimensional space, it is assumed that all heat exchangers in the thermal chimney are composed of circular cylinders.

Figure 9 shows the effect of horizontal pitches upon upward velocity of the thermal chimney with one row of condensers at 363 K (bottom) and one row of heaters at 423 K (top). The vertical pitch is kept at 2D. At large horizontal pitches cylinders tend to act independently, with the maximum velocity occurring within the thermal plume. As horizontal pitch decreases, interaction between cylinders qualitatively changes the flow field. The maximum upward velocity occurs in the throat between cylinders. Figure 10 shows area-averaged Nusselt number on the exterior surfaces of condenser cylinders and mass-averaged upward velocity at the bottom boundary with respect to different horizontal pitches. Variation of Nusselt number and upward velocity display similar trends, with an optimum value at P_h=1.75D for Nusselt number and P_h=2D for upward velocity. As the horizontal pitch declines, interaction between cylinders becomes stronger, which enhances natural draft, and blockage also gets stronger, which undermines natural draft. The trade-off between interaction and blockage produces an optimum value at P_h=1.75D.

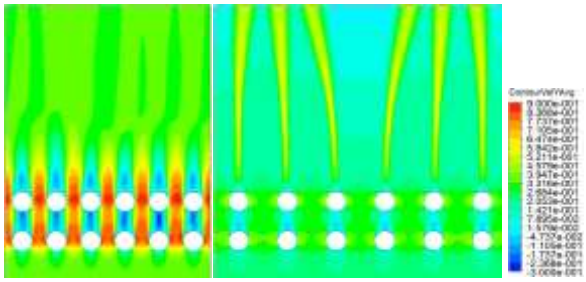

P_h=1.5D P_h=2D

Figure 9: Contour of upward velocity for two horizontal pitches (P_h).

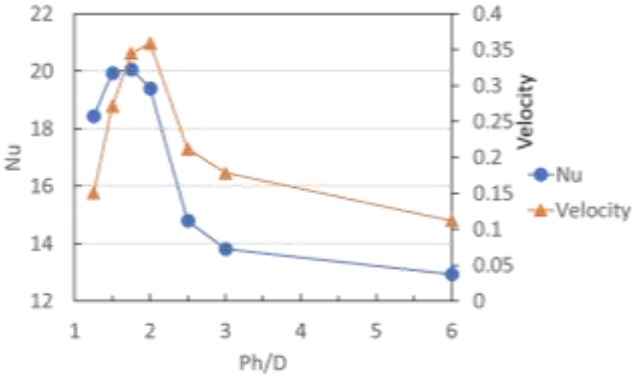

Figure 10: Area-averaged Nusselt number on the exterior of air-cooled condenser tubes and mass-averaged upward velocity at the bottom boundary.

Keeping the number of rows in the air-cooled condenser to one, the effect of increasing the number of rows in the air heater was also studied. Horizontal and vertical pitches were kept at their respective optimal values. Figure 11 shows the variation of area-averaged Nusselt number on the exterior of the condenser cylinders and mass-averaged upward velocity at the inlet with respect to number of cylinder rows in the air heater. As expected, natural draft strength and Nusselt number increase with more rows of air heater tubes due to greater energy input. Under the height constraint of the planned experimental rig, the optimum design was determined to be 18 cylinder rows in the air heater. The maximum heat transfer coefficient on the exterior surfaces of the air condenser at this value is 19 W/m^2-K. The maximum upward velocity at the inlet is 0.49 m/s. Compared with Lu et al. (2016), which reported an upward velocity of 0.35 m/s by natural draft from finned-tube

heat exchanger with similar temperature difference, the performance of our thermal chimney design is notably better.

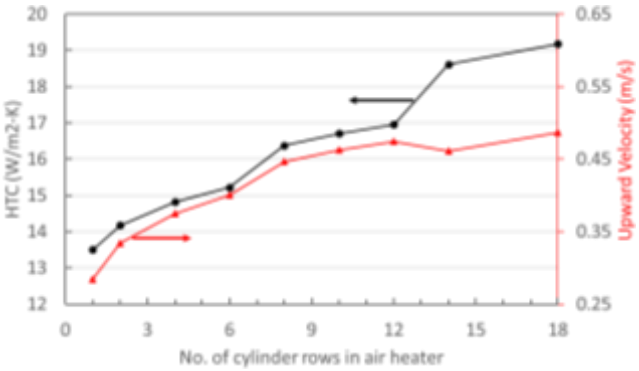

Figure 11: Area-averaged HTC on the exterior of air-cooled condenser tubes and mass-averaged upward velocity at the bottom boundary

To validate the CFD modelling results, a prototype of the thermal chimney-based condensation test system has been designed and is currently under construction. Initial experiments will include a single isothermal tube test to determine thermal plume pattern and flow acceleration (Figure 12).

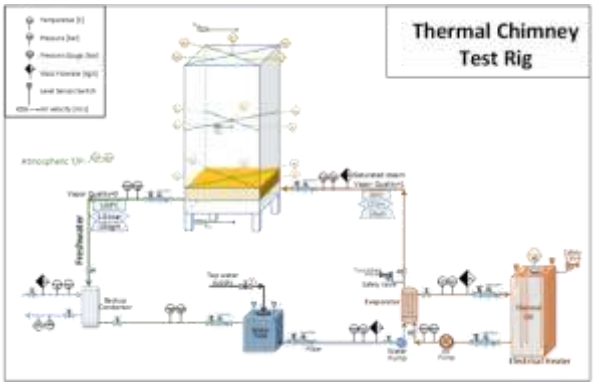

Figure 12: Schematic diagram of the thermal chimney driven air-cooled condenser test rig.

Interaction experiments between the air heater tubes and the condenser tube will then be conducted. Experimental feedback will allow for optimization of the test rig and CFD models and robust determination of thermal chimney effects, heat transfer enhancements and freshwater generation potentials.

5. CFD MODELLING AND ANALYSIS OF TWO-PHASE TURBINE

In the context of mechanical power generation from geothermal fluids, an impulse type steam turbine has been a classical approach. The systems employing binary fluids, such as organic fluids, have found use in low temperature heat sources due to their flammability at higher temperature. In high temperature sources, the brine is initially flashed and produced steam is used to drive the turbine. The total-flow concept which directly uses the brine as the turbines working fluid is the most efficient means of energy conversion but suffers from the backdrop of heavy mechanical erosion of the turbine, nozzle and mineral deposition which eventually leads to system failure. Austin et al. (1973) have presented the total-flow concept for power recovery for application to the Salton Sea geothermal bed. Hot brine was allowed to expand from 300 ℃, 2200 psia to 400 psia. Thermal energy was converted to kinetic head by expansion through a converging-diverging nozzle. The jet was then used to drive an impulse turbine. Similar concepts can be found in literature that have used multi-phase nozzles. Elliot (1982) has reported tests with water and nitrogen mixtures and with single stage and two stage impulse turbines. A special two-phase nozzle with mixer housing and liquid injection tube was designed to vary the mass ratio of liquid to vapour in the two-phase flow investigation. More recently Date et al. (2015) have presented experimental results of a curved nozzle total flow reaction turbine for low temperature feed water application. Curved nozzle design was based on the curvature calculation procedure described in Fabris (1993) with variable circular cross section such that pressure drop along the length of the diverging section is assumed to be linear and the change in relative velocity of the fluid along the length of the nozzle is also assumed to be linear. Two-phases tend to separate within the curved nozzle due to the large lateral acceleration and by designing the nozzle curvature using these assumptions, the lateral acceleration components of Coriolis acceleration, centripetal acceleration relative to motion and centripetal acceleration with respect to turbine axis can be balanced. Date et al. (2015) have reported test results from two operating feed water temperatures, for first test the average feed water temperature was maintained around 97 ℃ under local atmospheric pressure, and for the second test the average feed water temperature was maintained around 117 ℃. For both the tests the initial condenser pressure was maintained at around 6 kPa. The maximum power output of the turbine was estimated to be around 1330 W with an isentropic efficiency of around 25%.

5.1 Turbine Design

In the Combi-Gen project, the test turbine data presented by Date et al. (2015) has been used as a basis to establish a valid two-phase CFD model of the turbine. Figure 13 shows the lateral plane section of the reference turbine. The throat of the nozzle is 2.0 mm in diameter and located at a radial position of 59.15 mm from the axis of rotation. Nozzle cross section is circular and area function is defined by a variable diameter along the nozzle axis. The rotor is made out of Aluminium, has a diameter of 300 mm and the feed water is channelled axially into the two nozzles.

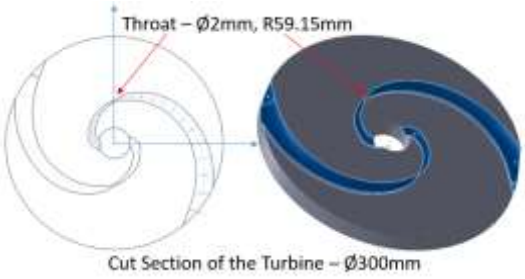

Figure 13: Reference Curved nozzle turbine geometry for CFD model development.

5.2 CFD Two-Phase Turbine Model

A Thermal Phase-Change model has been used in the CFD setup to solve the flash boiling of geothermal water in the expansion section of the turbine. This model defines the mass transfer due to flashing entirely based on the interphase heat transfer and overall heat balance at the phasic interface. At the water-liquid and water-vapour interface heat balance gives;

$$Q_w + Q_v = 0 \quad [1]$$

From the interface to water-liquid phase;

$$Q_w = \mathfrak{h}_w A_i (T_{sat} - T_w) - \dot{m}_{wv} \cdot H_{ws}$$

From the interface to water-vapour phase;

$$Q_v = \mathfrak{h}_v A_i (T_{sat} - T_v) + \dot{\boldsymbol{m}}_{\boldsymbol{wv}} \cdot H_{vs}$$

Sub-script s is selected depending on evaporation or condensation;

$$\mathfrak{h}_w A_i (T_{sat} - T_w) - \dot{m}_{wv} \cdot H_{ws} + \mathfrak{h}_v A_i (T_{sat} - T_v) + \dot{m}_{wv} \cdot H_{vs} = 0$$

$$\dot{m}_{wv} = \frac{\mathfrak{h}_w A_i (T_{sat} - T_w) + \mathfrak{h}_v A_i (T_{sat} - T_v)}{H_{vs} - H_{ws}}$$

The interphase mass transfer is obtained from equation [1]. Equations [2] and [3] are used to select the enthalpy for source in equation [1].

If $\dot{m}_{wv} > 0$ (Boiling),

$$H_{ws} = H_w(T_w)$$
$$H_{vs} = H_v(T_{sat}) \quad [2]$$

If $\dot{m}_{wv} < 0$ (Condensation),

$$H_{ws} = H_w(T_{sat})$$
$$H_{vs} = H_v(T_v) \quad [3]$$

$$L = H_v(T_{sat}) - H_w(T_{sat}) \quad [4]$$

As seen from equation [1], heat transfer coefficients $\mathfrak{h}_w$, $\mathfrak{h}_v$ and interfacial area A_i are required to be determined in the Thermal Phase-Change model. These inputs are prescribed by specifying the interface Nusselt numbers using test correlations available in the literature. The turbine has two symmetrically positioned curved nozzles. In order to reduce the CFD domain, a 180 degree sector of the rotor is modelled with periodic boundaries. Figure 14 presents the turbine flow domain and the computational mesh.

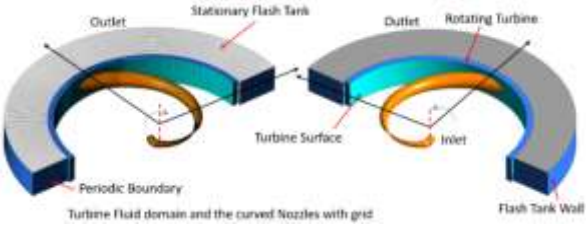

Figure 14: Turbine flow domain and computational mesh of the CFD model.

The inlet to the nozzle is defined by the feed water pressure of 400 kPa and temperature of 117 ℃. The exit of the turbine is open to a flash tank connected to condenser coil which during the start of the experiments is vacuum conditioned to 6 kPa pressure. Water fluid properties are defined using IAPWS-IF97 database. A table range is defined for the operating condition of the turbine in order to clip the properties during computations.

5.3 Turbine Analysis Results

CFD calculations were performed over a range of turbine operating speed from 1500 to 4600 rpm. This was the speed at which highest power output has been reported in Date et al. (2015). Figure 15 presents the distribution of pressure close to the throat of the curved nozzle. In order to resolve the contour plot a limited scale of 3 to 6 kPa has been applied to the plots. In the converging section the pressure is high until the nozzle throat. On the downstream of the throat a severe drop in local pressure is observed to about 2.93 kPa.

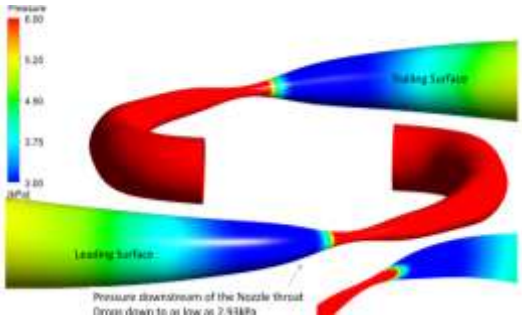

Figure 15: Pressure distribution at 4623 rpm on the curved nozzle scaled to a maximum of 6 kPa.

Further downstream the pressure recovers and is in the range of 4.5 to 15 kPa till the nozzle exit. Only a small difference in pressure is observed between the leading and trailing surface of the nozzle thus indicating a low torque from the expansion.

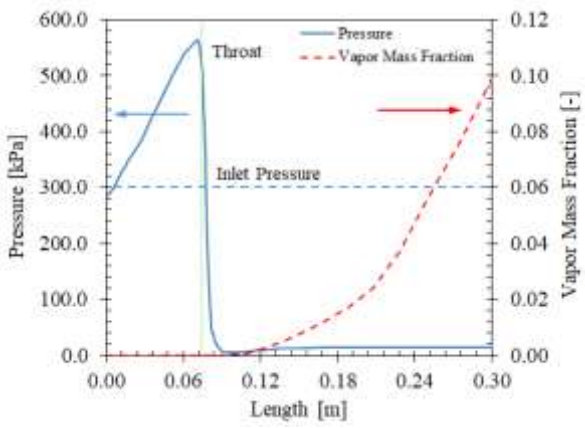

Figure 16: Evolution of pressure and vapour mass fraction at 4623 rpm along the axis of the curved nozzle in midplane.

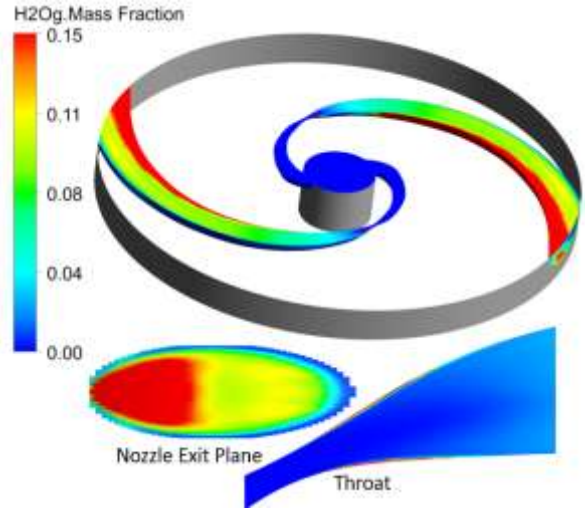

Figure 17: Local variation of vapour mass fraction in the turbine midplane and nozzle exit plane at 4623 rpm.

Figure 16 presents the evolution of pressure along the axis of the curved nozzle in turbine midplane. The inlet boundary to the nozzle is specified as 300 kPa. From inlet to the nozzle throat a steady increase in the fluid pressure is observed. Even though this is a converging section of the nozzle, the pressure rises due to rotational effect of the turbine. The peak pressure upstream of the nozzle goes up to 580 kPa and then severely drops down close to 3 kPa downstream of the nozzle throat. Using this information, the nozzle section could be redesigned in order to avoid the pressure rise which could improve the specific power output of the turbine.

Figure 16 also presents the variation of vapour mass fraction along the axis. From inlet to the throat, feed water remains in liquid state with no phase transition. At the throat the inception of water vapour due to flash boiling is observed in Figure 17. From the throat region and in the diverging section of the nozzle there is steady increase in vapour fraction. At nozzle exit the mass fraction is about 10%. A vapour quality of about 12.8% has been reported in the measurements and the CFD model prediction is close to the test results.

Analysis of the test turbine indicates the following performance response from the two-phase CFD model:

- Turbine flow at various operating speed was well estimated within 6 – 13% deviation from measurements.
- Nozzle torque and hence turbine power estimate was higher by 8 – 45% as compared to measurements.
- Turbine performance, liquid and vapour distribution and flash boiling boundaries were predicted by the analysis with turbine exit vapour mass fraction estimated in the range of the measurement of 12%.
- The model is responsive to operating condition and geometrical variation and hence can be used in future comparative design studies.

The CFD model will be used to design and optimize the two-phase turbine in Combi-Gen project.

6. CONCLUSIONS

The hydrogeochemical systematics of geothermal resources must be well understood if sustainable exploitation is to be achieved. Assessment of the chemical composition of geothermal source waters is also important for maintaining and optimising power production performance. In order to enhance the development of the Combi-Gen technologies, collection of hydrological and geological data from field sites in Kenya and Ethiopia is underway. This collection of new data is being complimented using existing published works on previous geothermal exploration efforts and active geothermal power plants across East Africa.

With respect to the design of combined power and freshwater generation technologies, higher turbine efficiencies result in beneficial system performance from every perspective. Higher temperature waters provide more efficient heat transfer and power production capabilities. Based on detailed distributed-parameter modelling and analysis, the design of the Combi-Gen system is selected to optimize both performance and operability. In order to reduce irreversibility and maximize the power output, an advanced total-flow reaction turbine has been designed. CFD modelling of the Combi-Gen thermal chimney driven air-cooled condenser demonstrates that the transition SST model provides the best solution for resolving the natural draft flow field.

It is observed that thermal plume accelerates as it develops and dissipates heat downstream. This interesting phenomenon is believed to be caused by buoyancy force within the thermal plume, manifested

by the increase of total pressure and decrease of temperature along the thermal plume. Furthermore, simulations on the natural draft within the thermal chimney demonstrate the existence of an optimum horizontal pitch between condenser pipes, due to the trade-off of interaction between cylinders and throat blockages. Using the expected dimensions of a future experimental rig, it is predicted that the optimum design includes 18 cylinder rows for the air heater, with maximum upward velocity of 0.49 m/s at the bottom boundary and a maximum 19 W/m^2-K heat transfer coefficient on the exterior surfaces of the air condenser cylinders.

A two-phase CFD model for calculation of flash boiling flows in nozzle and turbines was applied using the Thermal Phase-Change formulation in ANSYS CFX solver. The water properties database defined by IAPWS-IF97 was used to provide the fluid properties of both liquid and vapour phases. The two-phase CFD model has been adapted with moving reference frame, periodic boundary conditions, etc., and tested on a reference turbine geometry. The CFD model will be used further to design and optimize the two-phase turbine in Combi-Gen project to improve the specific power output. The outputs of the model will be further assessed, in combination with geothermal resource data to identify likely flow rates and phase conditions of 'spent' geothermal fuel which will be introduced into the Combi-Gen thermal chimney system. By integrating and optimizing cooling tower technology and solar thermal chimney technology, the Combi-Gen thermal chimney concept eliminates the parasitic power load of electric fans and avoids wasting extra cooling water.

This dual generation of power and production of fresh water aims to enhance the resource availability of energy-poor and water-short nations associated with the East African Rift System. The main focus of the Combi-Gen project is within Ethiopia and Kenya, but the potential application of the technology is not restricted to these countries. With appropriate knowledge of geothermal resource parameters, the Combi-Gen concept could ultimately be adapted for application in any geothermal setting.

REFERENCES

Abuaf, N., Wu, B. J. C., Zimmer, G. A., and Saha, P.: A study of nonequilibrium flashing of water in a converging-diverging nozzle. Lawrence Berkeley National Laboratory, (1981), BNL-NUREG/CR-1864, Volume 1.

Austin, A. L., Higgins, G. H., and Howard, J. H.: The total flow concept for recovery of energy from geothermal hot brine deposits. Lawrence Livermore Laboratory, (1973), UCRL-51366.

Biru, M.F.: Analysis of well testing, temperature and pressure in high-temperature wells of Aluto-Langano, Ethiopia. *Geothermal Training Programme 2016,* Reykjavik, Iceland, (2016), Number 13, 28 pp. https://orkustofnun.is/gogn/unu-gtp-report/UNU-GTP-2016-13.pdf accessed June 2018.

Burnside, N.M, Banks, D.B., and Boyce, A.J.: Sustainability of thermal energy production at the flooded mine workings of the former Caphouse Colliery, Yorkshire, United Kingdom. *International Journal of Coal Geology*, **164**, (2016), 85-91.

Corcione, M.: Correlating equations for free convection heat transfer from horizontal isothermal cylinders set in a vertical array. *International Journal of Heat and Mass Transfer*, **48 (17)**, (2005), 3660-3673.

Date, A., Vahaji, S., Andrews, J., and Akbarzadeh, A: Experimental performance of a rotating two-phase reaction turbine. *Applied Thermal Engineering*, **76**, (2015), 475-483.

Elliot, D. G.: Theory and Tests of Two-phase Turbines, Jet Propulsion Laboratory Publication, 81-105, (1982), DOE/ER-10614-1.

Fabris, G: Two-phase Reaction Turbine, United States Patent 5, 236, 349 (1993).

Geremew, H.: A Study of Thermodynamic Modelling and Gas Extraction System Design For Aluto Langano Geothermal Power Plant, Ethiopia, *Geothermal Training Programme 2012*, Reykjavik, Iceland, (2012), Number 10.

Grafsrønningen, S., Jensen, A., and Reif, B.A.P: PIV investigation of buoyant plume from natural convection heat transfer above a horizontal heated cylinder. *International Journal of Heat and Mass Transfer,* **54 (23-24)**, (2011), 4975-4987.

Hundy, G.F., Trott, A.R., Welch, T.C.: Refrigeration and air-conditioning, Butterworth-Heinemann, London, (2008).

Hotspur Geothermal: Cluff Geothermal was awarded the Fantale Geothermal Licence, situated around the prominent volcanic centre of Mt. Fantale near the town of Metehara, in July 2015, (2015) http://www.hotspurgeothermal.com/projects/ethiopia/fantale accessed February 2019.

IEA: Electricity generation by fuel. International Energy Agency, (2019) https://www.iea.org/statistics/?country=WORLD&year=2016&category=Electricity&indicator=ElecGenByFuel&mode=chart&dataTable=ELECTRICITYANDHEAT accessed Feb. 2019.

IRENA: Geothermal - Geothermal energy data. International Renewable Energy Agency (2019) https://www.irena.org/geothermal accessed February 2019.

Janet, J.P., Liao, Y., and Lucas, D.: Heterogeneous nucleation in CFD simulation of flashing flows in converging–diverging nozzles. *International Journal of Multiphase Flow*, **74**, (2015), 106–117.

Kagiri, D.: KenGen Power Africa Geothermal Road Show, September 2014.

Kenyan Government: Nationally Appropriate Mitigation Action (NAMA) to accelerate geothermal power: Lessons from Kenya. *Climate and Development Knowledge Network,* (2014).

Kitamura, K., Mitsuishi, A., Suzuki, T., and Kimura, F.: Fluid flow and heat transfer of natural convection induced around a vertical row of heated horizontal cylinders. *International Journal of Heat and Mass Transfer* **92**, (2016), 414-429.

Kuehn, T.H., and Goldstein, R.J.: Numerical solution to the Navier-Stokes equations for laminar natural convection about a horizontal isothermal circular cylinder. *International Journal of Heat and Mass Transfer*, **23 (7)**, (1980), 971-979.

Liao, Y., and Lucas, D.: 3D CFD simulation of flashing flows in a converging-diverging nozzle. *Nuclear Engineering and Design*, **292**, (2015), 149–163.

Lu, Y., Guan, Z., Gurgenci, H., Alkhedhair, A., and He, S.: Experimental investigation into the positive effects of a tri-blade-like windbreak wall on small size natural draft dry cooling towers. *Applied Thermal Engineering,* **105**, (2016), 1000-1012.

Lysak, S.V.: Heat flow variations in continental rifts. *Tectonophysics*, **208 (1-3)**, (1992), 309-323. doi: 10.1016/0040-1951(92)90352-7

Noto, K., Teramoto, K., and Nakajima, T.: Spectra and critical Grashof numbers for turbulent transition in a thermal plume. *Journal of thermophysics and heat transfer,* **13 (1)**, (1999), 82-90.

Owen, R., MacNaghten, P., and Stilgoe, J.: Responsible research and innovation: From science in society to science for society, with society. *Science and Public Policy*, **39**, (2012), 751–760.

Reddy, K. V., and Ghaffour, N.: Overview of the cost of desalinated water and costing methodologies. *Desalination*, **205 (1)**, (2007), 340-353. doi: 10.1016/j.desal.2006.03.558

Saitoh, T., Sajiki, T., and Maruhara, K.: Bench mark solutions to natural convection heat transfer problem around a horizontal circular cylinder. *International Journal of Heat and Mass Transfer*, **36 (5)**, (1993), 1251-1259.

Tadesse, F.: Ethiopia: Aluto-Langano geothermal expansion comes to life. *Addis Fortune*, **18(934)**, (2018), 18th March 2018. https://addisfortune.net/articles/aluto-langano-geothermal-expansion-comes-to-life/ accessed Feb. 2019.

Teklemariam, M. and Beyene, K.: Geochemical monitoring of the Aluto-Langano Geothermal field. *26th Workshop on Geothermal Reservoir Engineering*. Stanford University, Stanford, California, USA, (2001), 29th-31st January 2001.

Tibebu, H.: Ethiopia: Geothermal sites with over 10,000 MWs potential discovered in Rift Valley. *The Ethiopian Herald*, (2018), 24th March 2018. https://allafrica.com/stories/201803260706.html accessed February 2019.

Tingzhen, M.: Solar Chimney Power Plant Generating Technology, Zhejiang University Press, Zhejiang, (2016).

Wang, P., Kahawita, R., and Nguyen, T.H.: Numerical computation of the natural convection flow about a horizontal cylinder using splines. *Numerical Heat Transfer*, **17 (2)**, (1990), 191-215.

WHO, Drinking-Water, Fact sheet N°391, June 2015.

Younger, P.L.: Reconnaissance assessment of the prospects for development of high-enthalpy geothermal energy resources, Montserrat. *Quarterly Journal of Engineering Geology and Hydrogeology*, **43**, (2010), 11–22.

Acknowledgements

The Combi-Gen project is funded by EPSRC GCRF grant EP/P028829/1. The authors are grateful to the late Prof Paul Younger for his inspiration and kinship. We are also thankful to Dr Abhijit Date, RMIT, Australia, for providing reference turbine test data for development and validation of CFD models.

Author Contributions

Manuscript prepared by NB (Project Co-I; WP3 lead) with written section contributions led by SR (5), GY (3) and HM (4). NM and WL provided additional input throughout. Further contributions from ZY (Project PI; WP1 lead), LH (Co-I; WP2 lead), ELT (Co-I) and AB (Co-I).